Overview of various machines, experiments at COSY

1. Methods of the friction force measurements
1.1. Longitudinal component
1.2. Transverse component
2. Determination of the electron beam temperature
3. Dependence on magnetic field value
4. Dependence on electron temperature
5. Scaling with charge number
6. Magnetic field imperfection (?)
7. COSY cooler
8. Field quality
9. Beam manipulation
10. Friction force measurements
11. Possible experiments

1.1. Longitudinal cooling

Four general methods

Rang of the ion velocity 0 – 10^4 m/s

1. Equilibrium between a longitudinal heating of the ion beam and electron cooling

$$F_{\|}(v) = D\,\frac{\partial\rho/\partial v}{\rho(v)}$$

Developed at LEAR (H.Poth et al., NIM A 287(1990), 328) improved and calibrated at ESR (T.Wincler et al., Hiperfine Int. 99 (1996) 227)

2. Equilibrium between induction acceleration and electron cooling (TSR, HIMAC)

3. Phase shift method

Equilibrium between cooling and RF acceleration

$$F_{\parallel} = Ze\hat{U}_{rf} \sin \Delta\phi_s$$

(bunched ion beam)

Rang of the ion velocity $10^4 - 10^7$ m/s

4. Voltage step method

$$F_{\parallel} = \frac{p}{\eta} \frac{df/dt}{f}$$

1.2. Transverse cooling

1. Measurements of the beam profile during cooling

C. Carli, M. Chanel, Bad Honnef conference, LEAR - LEIR
The profiles are transformed in amplitude density distributions by applying an Abel transformation.
(M. Chanel, NIM A 441 (2000) 64 –69)

M. Beutelspacher et al. NIM *A 441 (2000) 110-115, TSR*

$$\frac{1}{\sigma_j}\frac{\mathrm{d}\sigma_j}{\mathrm{d}t} = -\frac{1}{\tau_j} + \lambda$$

2. Damping time of coherent oscillations

3. Measurement of the maximum position

H. Danared et al. NIM *A 441 (2000) 123-133 (CRYRING)*

Transverse “chromatic” instability will occur when a misalignment introduced between the ion and the electron beam exceeds the velocity where the transverse friction force has its maximum.

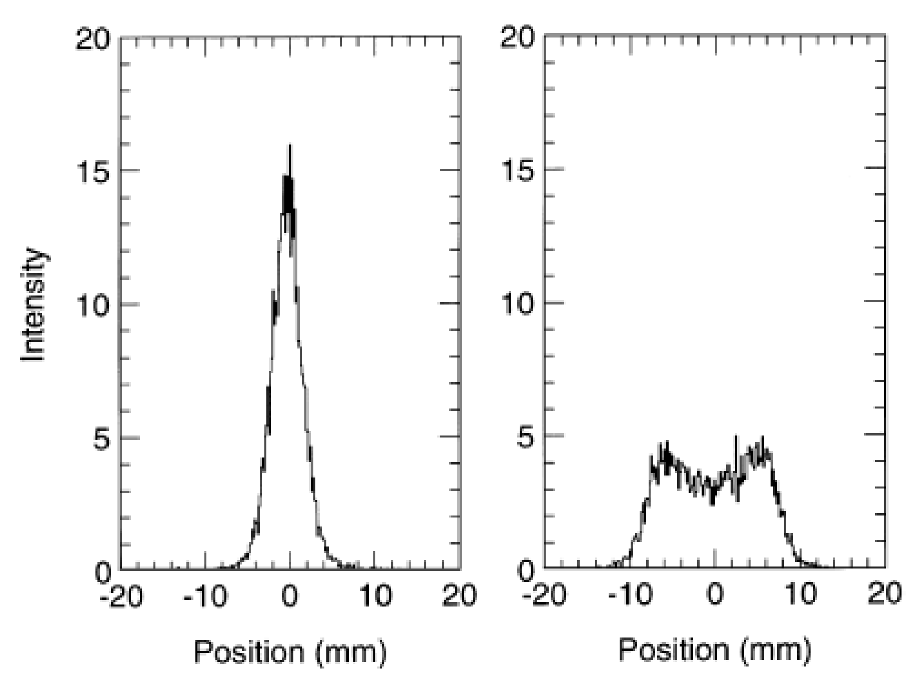

Fig. 9. Profiles of a cooled ion beam with well-aligned electrons (left) and of a beam above the instability threshold where the electron beam was misaligned by 2.3 mrad (right).

2. Determination of the electron beam temperature

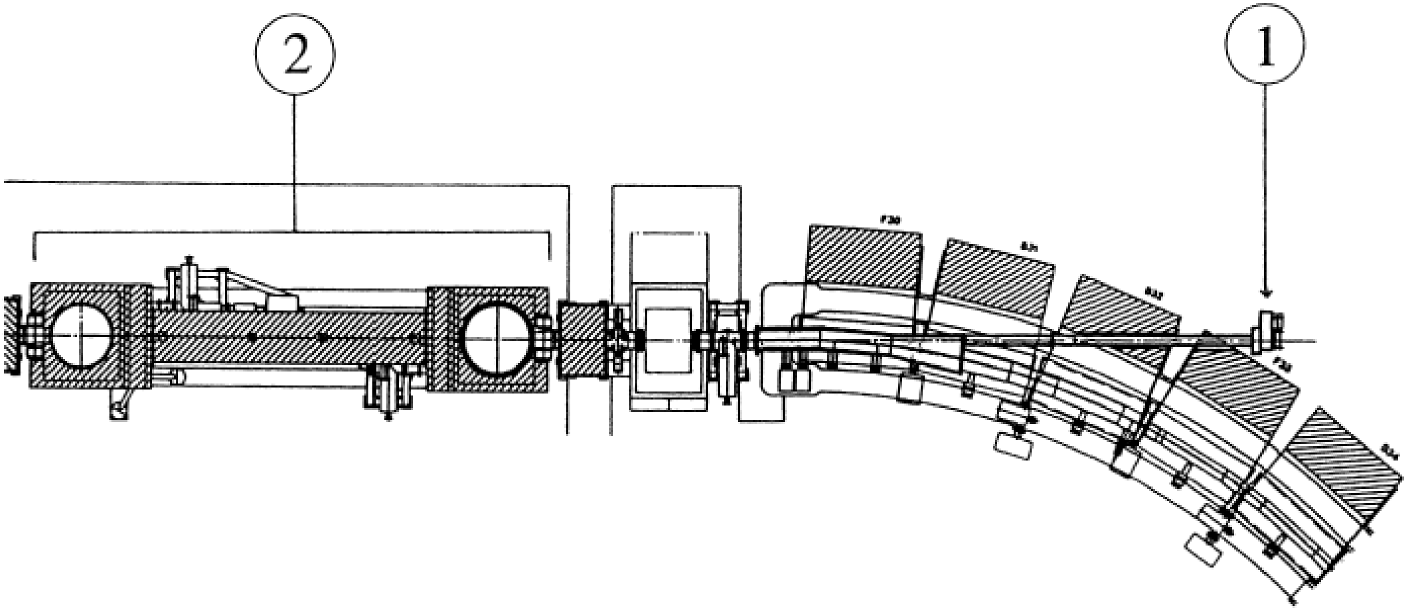

Fig. 1. Drawing showing the position of the H^0 profile monitor (1) straight after the electron cooler (2).

T. Bergmark et al. NIM *A 441 (2000) 70-75, CELSIUS*

$$\alpha_{RR} = 3.02 \times 10^{-13} \frac{\mathrm{cm}^3}{\mathrm{s}} q^2 \sqrt{\frac{\mathrm{eV}}{kT_\perp}} \times \left[\ln\left(\frac{11.32q}{\sqrt{kT_\perp/\mathrm{eV}}} \right) + 0.14 \left(\frac{kT_\perp}{q^2\mathrm{eV}} \right)^{1/3} \right]$$

A. Wolf et al., NIM *A 441 (2000) 183-190*
Heidelberg

H.Danared, NIM A 391 (1997) 24-31 CRYRING

$$\alpha_r(v_d) = \int \sigma(v) v f(\boldsymbol{v}_e)\, d^3 v_e$$

$$f(\boldsymbol{v}_e) = \frac{m_e}{2\pi k T_{e\perp}} \left(\frac{m_e}{2\pi k T_{e\parallel}} \right)^{1/2} \times \exp\left(-\frac{m_e v_{e\perp}^2}{2kT_{e\perp}} - \frac{m_e v_{e\parallel}^2}{2kT_{e\parallel}} \right)$$

If cross-section has a peak $\sigma = \sigma_0 \delta(E - E_0)$

$$\alpha_r(v_d) = \frac{\sigma_0 v_0}{2\lambda k T_{e\perp}} \exp\left[\frac{-m_e}{2kT_{e\perp}} \left(v_0^2 - \frac{v_d^2}{\lambda^2} \right) \right] \times \left[\mathrm{erf}\left(\sqrt{\frac{m_e}{2kT_{e\parallel}}} \frac{v_d + \lambda^2 v_0}{\lambda} \right) - \mathrm{erf}\left(\sqrt{\frac{m_e}{2kT_{e\parallel}}} \frac{v_d - \lambda^2 v_0}{\lambda} \right) \right].$$

$$\lambda = (1 - T_{e\parallel}/T_{e\perp})^{1/2}$$

A process that cross-sections can be regarded as delta function - dielectronic recombination

Accuracy for transverse temperature ~ 1%

3. Dependence on Magnetic field value

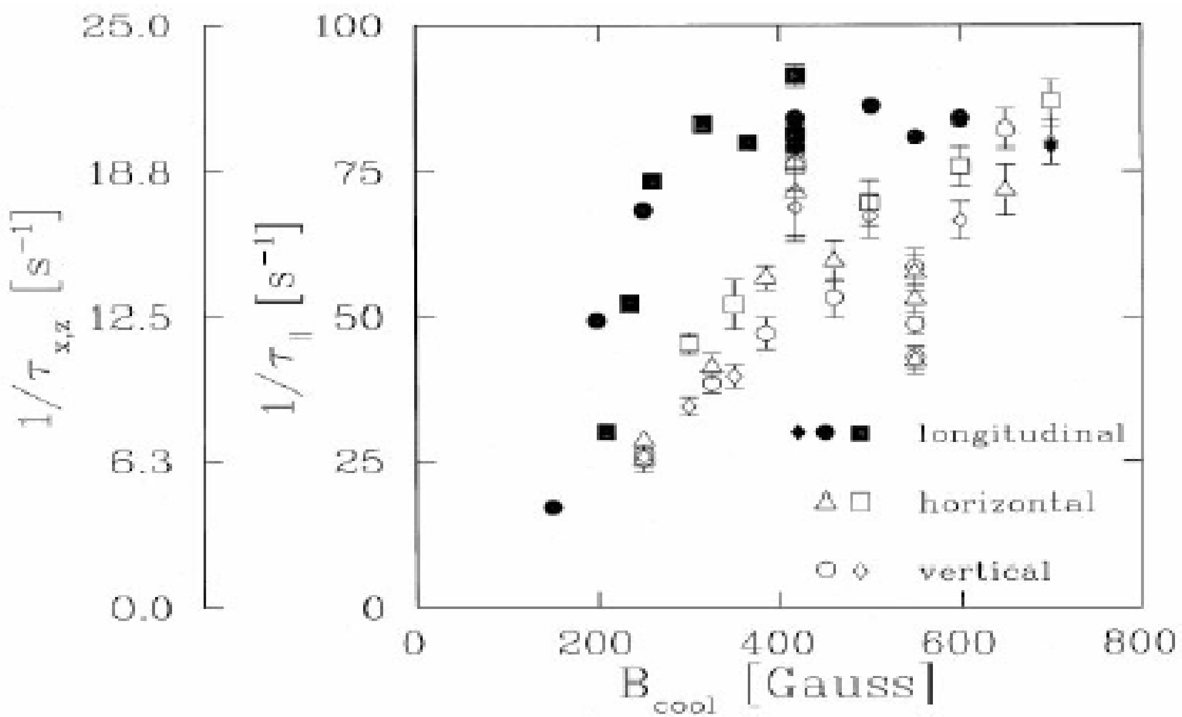

Fig. 5. Cooling rates $1/\tau_{\parallel}$ and $1/\tau_j$ as functions of the magnetic field in the interaction region (ion current 20 μA, expansion factor 9.6, electron density 8.0×10^6 cm^{-3}). Different plotting symbols result from different beam times.

TSR $^{12}C^{6+}$ ions at energy of 73.3 MeV

(At ESR in the range 1.1-1.5 kG there is no dependence)

M. Beutelspacher et al. NIM *A 441 (2000) 110-115, TSR*

4. Dependence on electron transverse temperature

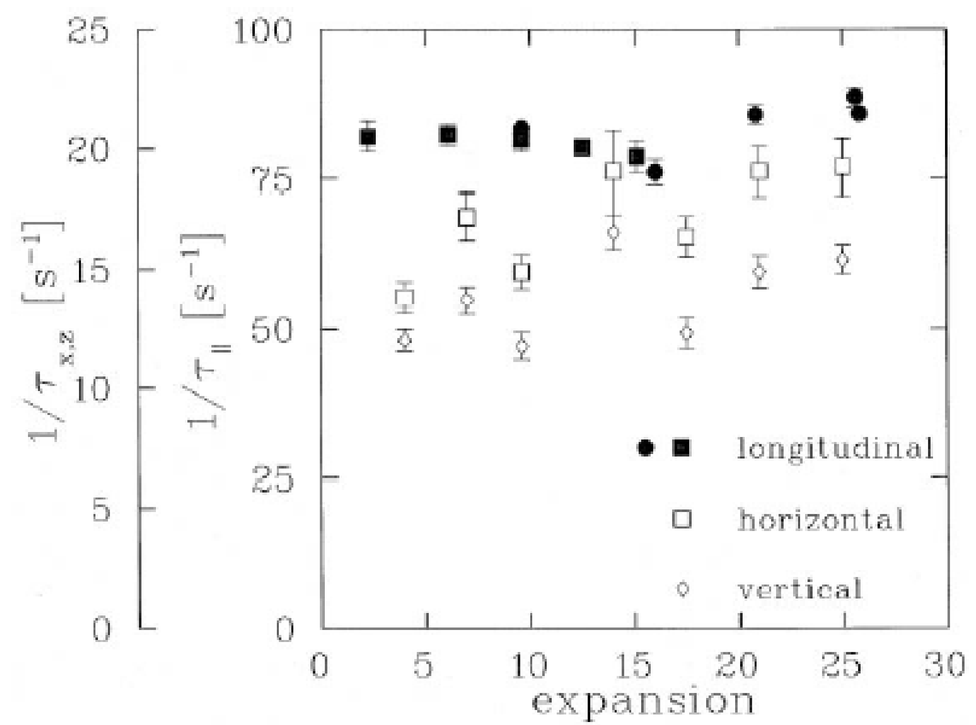

Fig. 6. Cooling rates $1/\tau_{\|}$ and $1/\tau_j$ as functions of the expansion factor ($B_{cool} = 418$ G, $n_e = 8.0 \times 10^6$ cm^{-3}, ion current 20 μA). Different plotting symbols result from different beam times.

M. Beutelspacher et al. NIM *A 441 (2000) 110-115, TSR*

5. Scaling with charge number

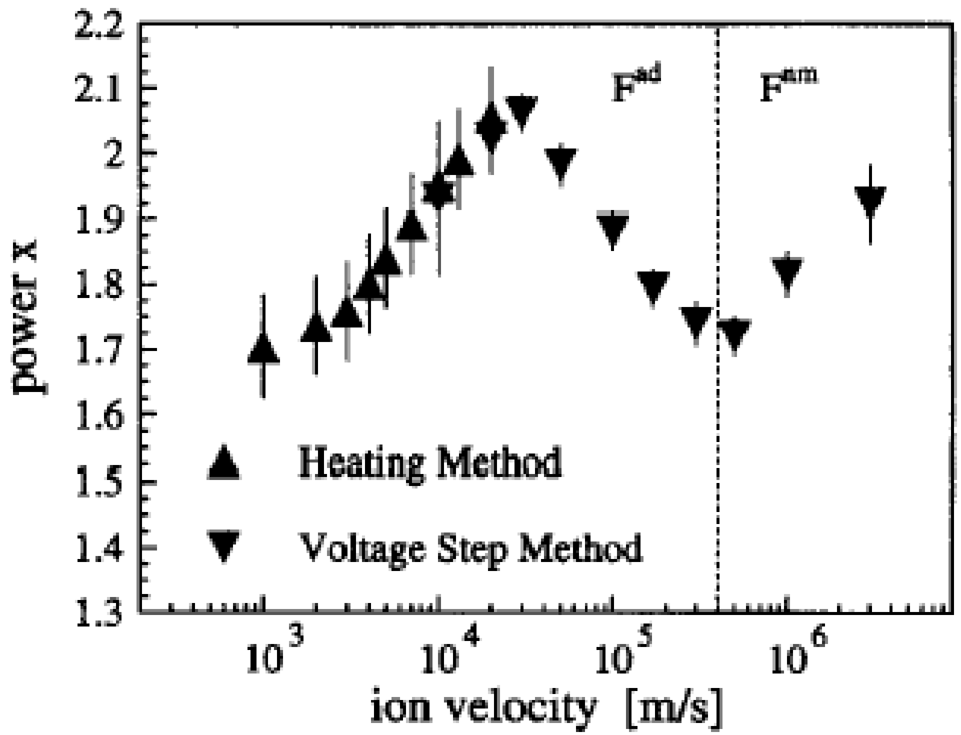

Fig. 3. Variation of the power of the charge scaling of the longitudinal cooling force with the ion velocity.

ESR
Longitudinal force
Ions from $^{12}C^{6+}$ to $^{238}U^{92+}$
Energy range 50-370 MeV/u

RHIC

$$V_s = \beta c(\Delta p/p) \approx$$

$$3 \cdot 10^5 \ m/sec$$

T.Wincler et al., NIM A391 (1997) 12-16

7. COSY cooler

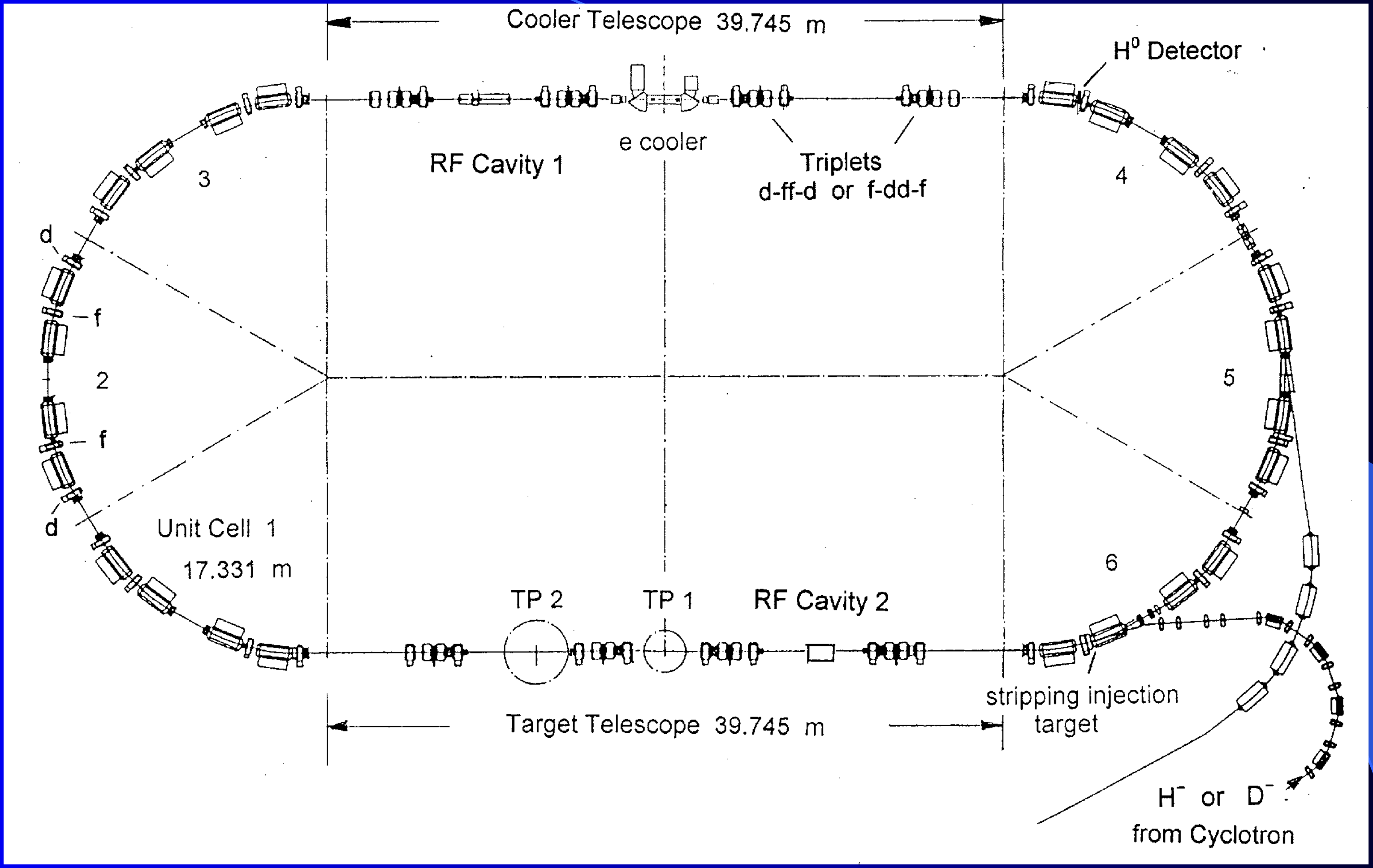

Injection energy 45 MeV for protons, electron energy ~ 24.5 keV

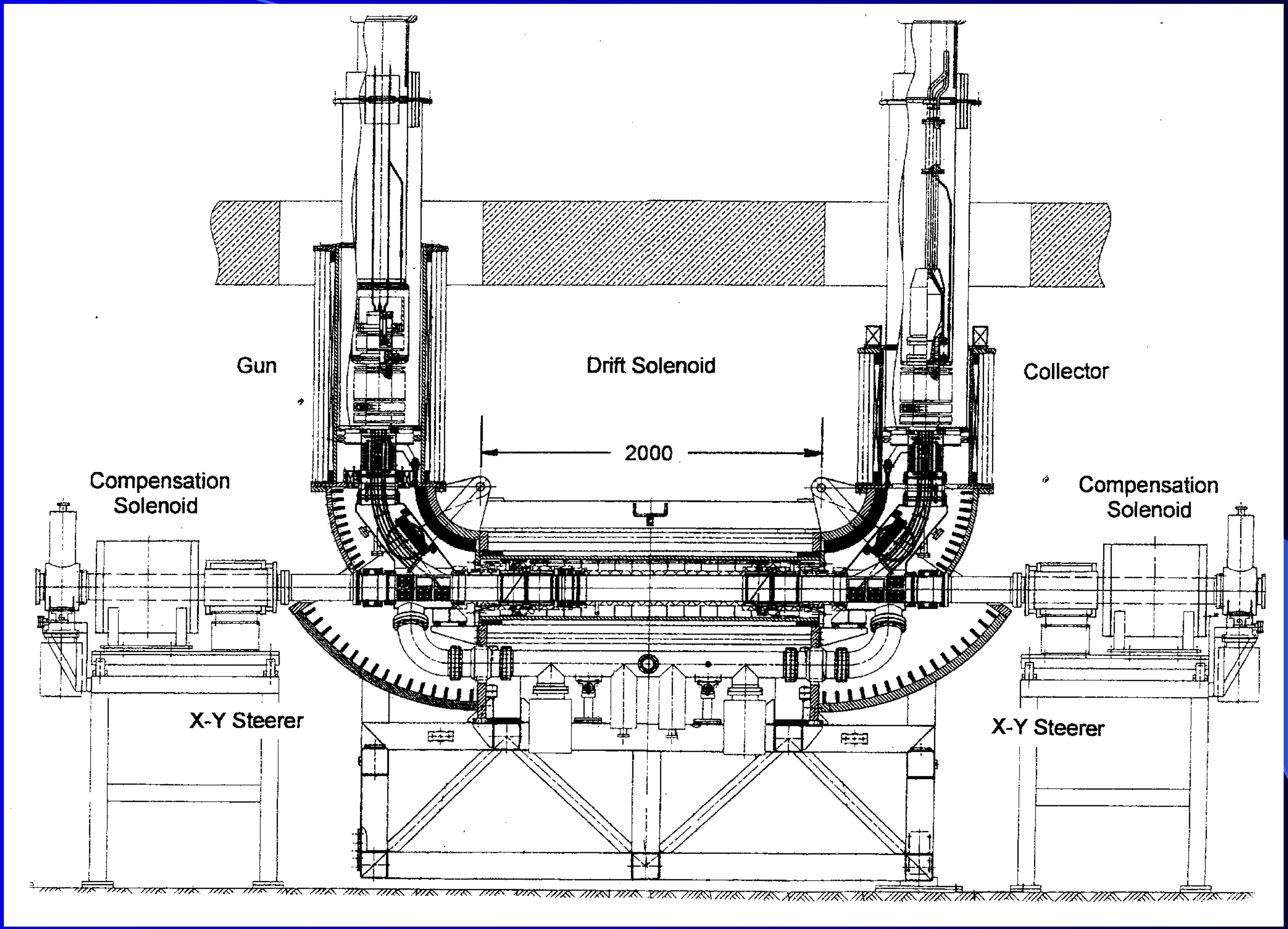

Length of the proton beam orbit inside magnetic field ~ 3m

Length of the straight solenoid 2m

“Effective” length of the cooling section 1.4 m

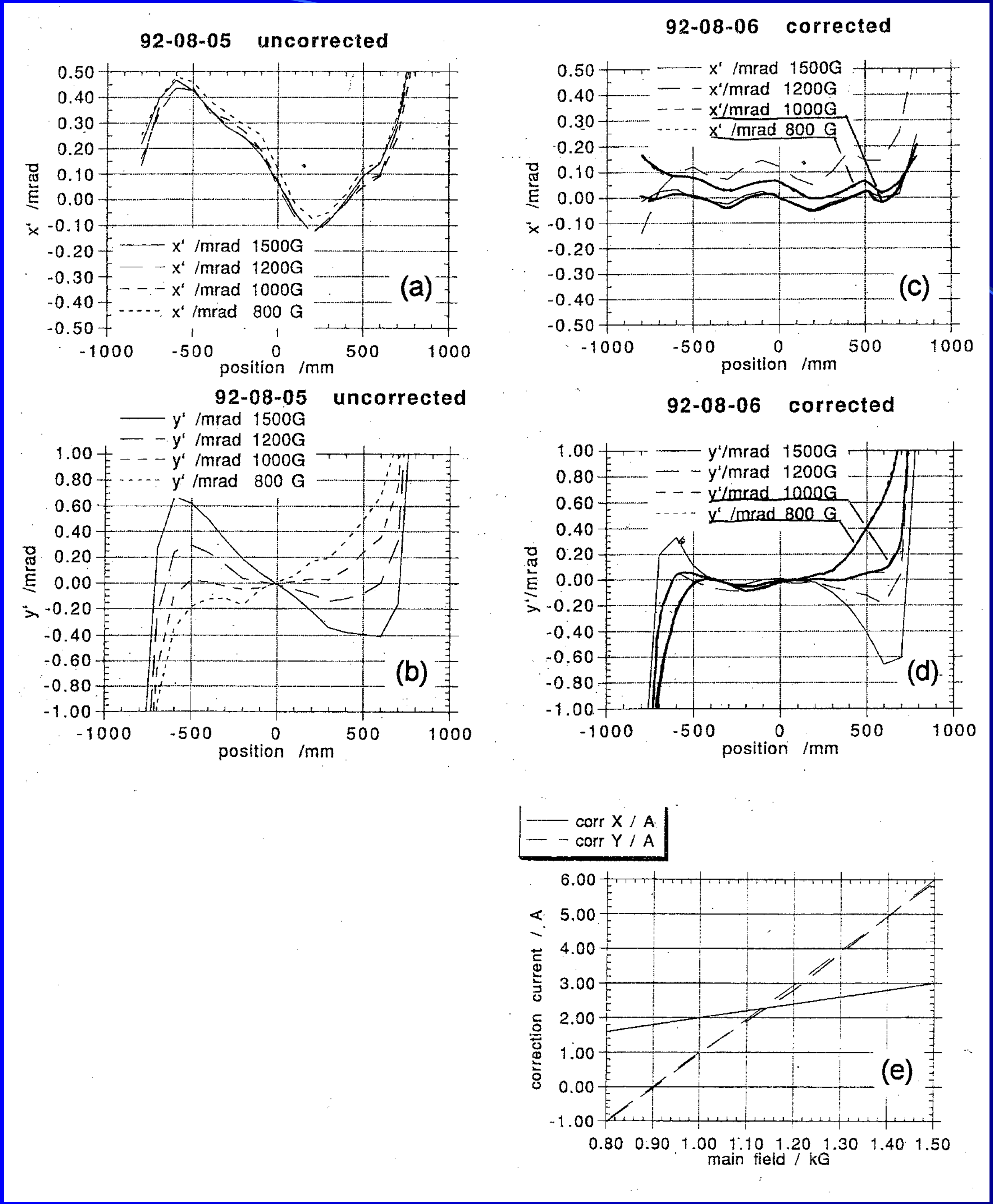

1992 – assembly and test
1993 – displacement to nominal position, first cooling
199? – discovery of "tower wall" instability during stacking and "electron heating" effect,
May 2001 – first ecool run
December 2001 – work for experiment

General goals :

-decrease initial momentum spread for effective adiabatic bunching and further acceleration,

-decrease emittance for effective fast extraction after acceleration,

-suppress the halo for slow extraction,

-increase of the polarized beam intensity using stacking-cooling procedure.

9. Beam manipulation

Gun, drift, and collector solenoid are equipped with steering coils for both directions.

The coils produce a transverse magnetic field so that the longitudinal field lines get inclined. Since the electrons follow the longitudinal field lines, steering at the gun solenoid results in a displacement of the electron beam in the drift solenoid. Then, the collector steering has to be in opposite direction in order to guide the beam into the collector.

The drift solenoid steering is used for the orientation of the electron beam.

The effectiveness of the gun steering at 800 G longitudinal field was measured to be 1.54 mm/A, that of the drift steering 0.7 mrad/A.

Displacements of ± 10 mm and orientation angles of ± 2 mrad can be applied at the same time without hitting the potential tubes in the toroids

Diagnostics

The neutral particle detector (H^0 detector)

main tool to find the necessary ion
and electron beam settings for cooling

is mounted in a distance of 24.3 m downstream the center of the drift solenoid.

It consists of two crossed wire chambers for profile measurements, (wire distance 1 mm) and two scintillators behind operated in coincidence for measuring absolute rates.

The repetition rate of the wire chamber spectra is about 2 s.
The acceptance of the H^0 detector is ± 1 mrad.

Beam alignment

The minimum of the angular divergence between electron and proton beam can be found via measurements:

- the dumping time (total cooling time at the same step of the cathode voltage),

- profile width,

- H^0 count rate

as functions of the electron beam angle.

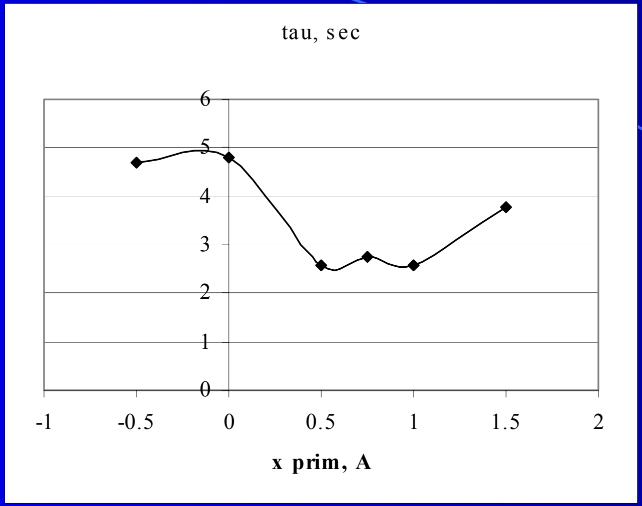
tau, sec
x prim, A

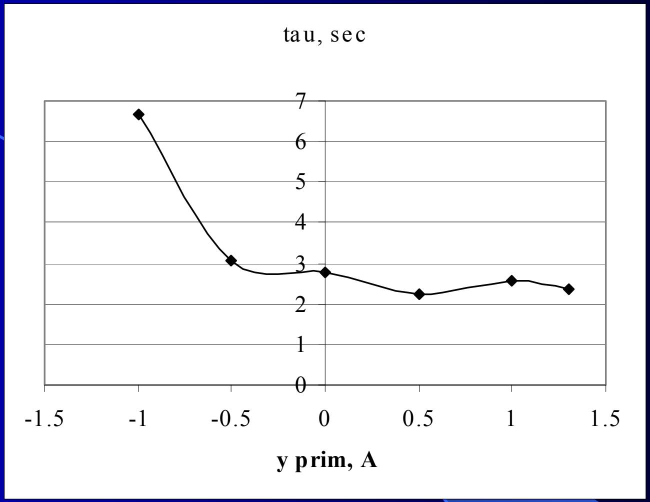
tau, sec
y prim, A

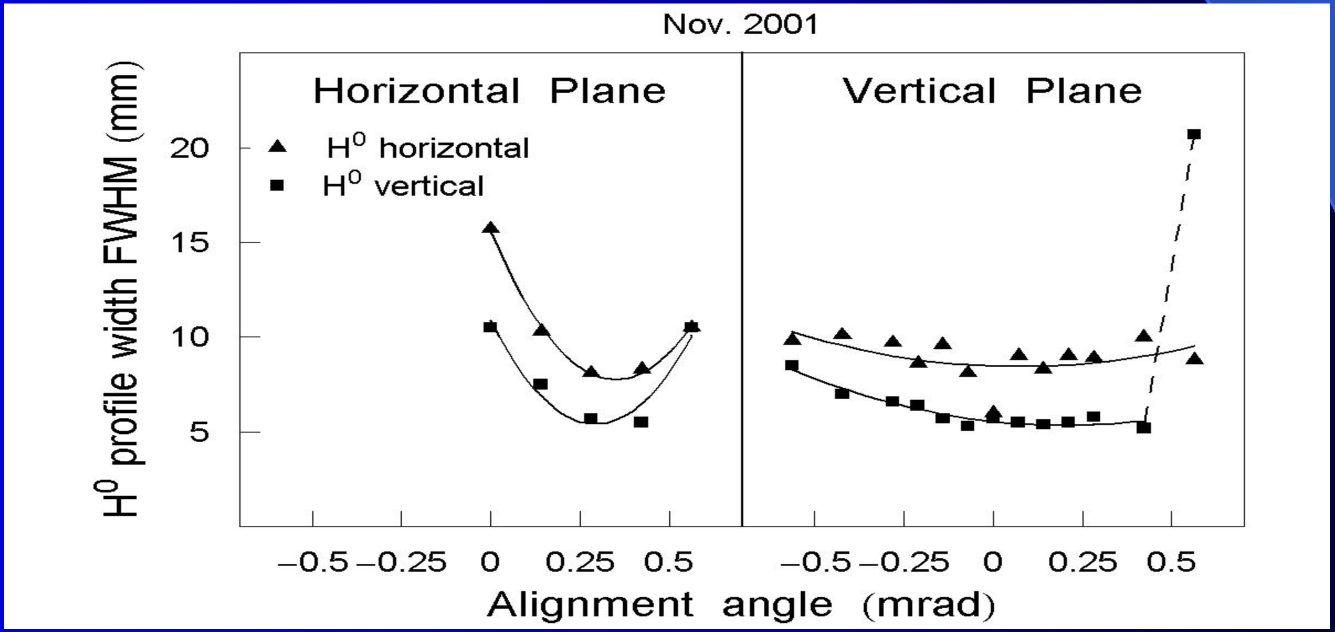
Nov. 2001
Horizontal Plane
Vertical Plane
H0 horizontal
H0 vertical
H0 profile width FWHM (mm)
Alignment angle (mrad)

Correction coils is out of operation.

Electron temperature, determined through the recombination rate

$T_{\perp,eff} \sim 300$ meV

Chromatic instability is absent,
maximum misalignment angle ±0.7 mrad:
Effective temperature corresponding to maximum of the friction force

$T_{eff} > 20$ meV

Friction force measurement using voltage step method

After fast change of the cathode voltage the revolution frequency is measured as a function of time

$$F_{\parallel} = \frac{l_e}{C}\frac{p}{\eta}\frac{df/dt}{f}$$

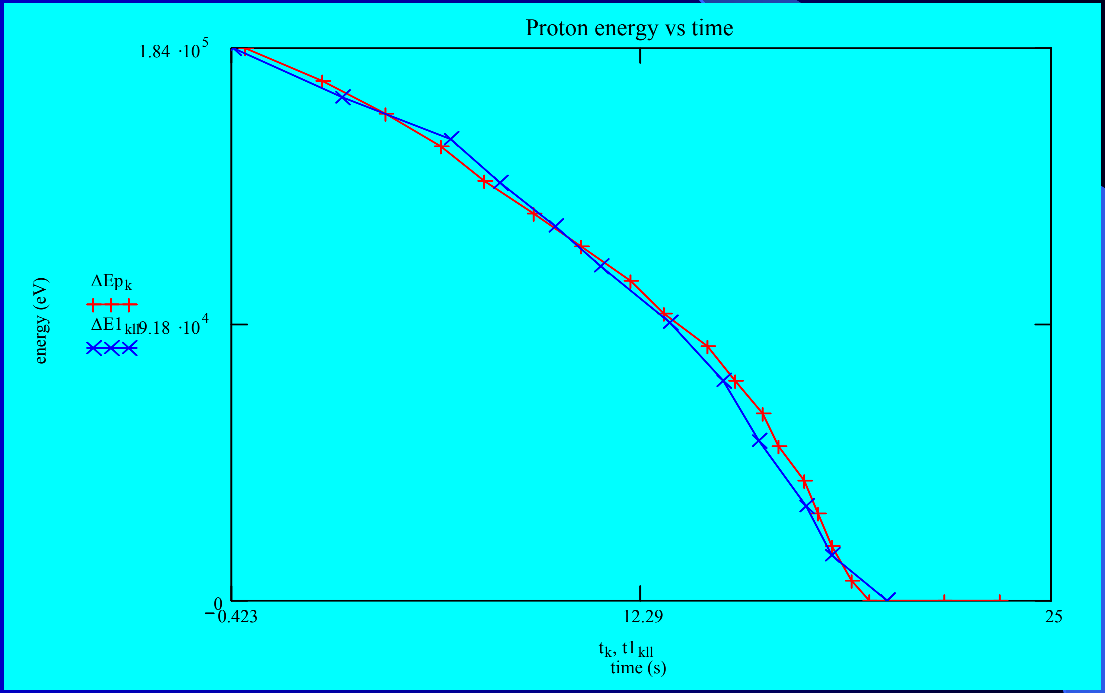

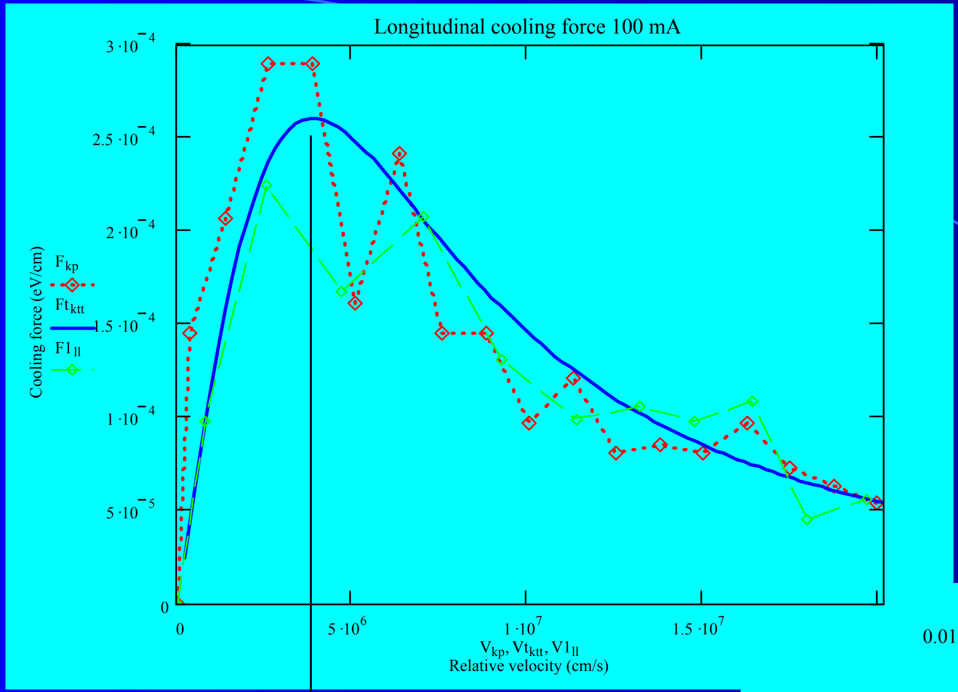

$$F(V) = mc^2 \frac{4r_e^2 n_e L n_c}{(V^2 + V_{eff}^2)^{3/2}} V$$

$\sim 4 \cdot 10^4$ m/s

$T_{eff} \sim 15$ meV

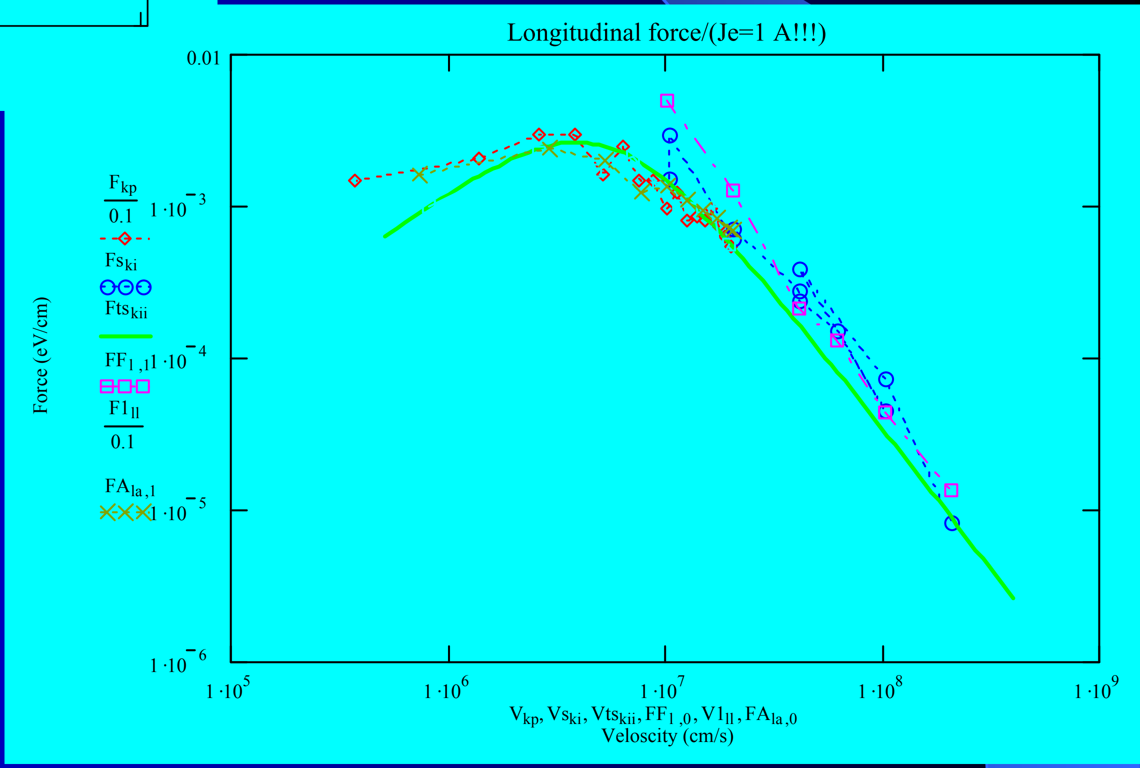

11. Possible experiments

1. Dependence of the friction force on magnetic field value:
There is a possibility to change the field in all the solenoids simultaneously from 400 to 1200 G

2. Dependence on longitudinal temperature (?):
Artificial increase of the cathode power supply noise

3. Dependence on the field imperfection:
Measurements of the force with field correction, search for chromatic instability